Chapter 11
Utilization of Stone Industry Waste as Filler for Sustainable Development of Aluminum Alloy Composites: A Thermo-Mechanical and Mechanical Characterizations

Vikash Gautam, Amar Patnaik, and I. K. Bhat

Introduction

Rapid development of industries and urbanization of place as well as rise in the living standards of people is the root cause for the arise of a major problem of solid wastes. Industrialization is the necessity of developing countries to boost up nation's economy. Simultaneously, it is the root cause for the generation of a huge quantity of waste that led toward serious problem related to health or environmental pollution. Therefore, wastes are seemed to be a by-product of growth in industries. The waste products increase with the increasing demand for raw materials in industries and conventional resurfaces are diminishing day by day. Wastes occupy the land distorting its fertility, and simultaneously increase the cost of waste disposal. The developing countries like India need to make effort for minimization of these solid wastes and simultaneously recycle of the waste or utilization of waste in different areas. At the same time, the need for sustainable development program has all amplified the need to reuse the materials that were once regarded as wastes. Over recent decades, innovative research works have been carried out to explore all possible

V. Gautam (✉)
Mechanical Engineering Department, Swami Keshvanand Institute of Technology, Jaipur 302025, India
e-mail: Gautam.mnitj@gmail.com

A. Patnaik
Mechanical Engineering Department, Malaviya National Institute of Technology, Jaipur 302017, India

I. K. Bhat
Vice Chancellor at Manav, Rachna University, Faridabad, Haryana 121004, India

S. Kumar and K. P. Rajurkar (eds.), *Advances in Manufacturing Systems*,
Lecture Notes in Mechanical Engineering,
https://doi.org/10.1007/978-981-33-4466-2_11

methods for utilization of waste materials in wide range. Till now wastes generated through industrialization and urbanization have been used in many places as alternative aggregates in embankment, road, pavement, and building construction.

Various solid wastes are generated by the industries such as copper slag, alumina, fly ash, cement by pass dust (CBPD), cement klin dust, and rice husk. Copper slag is a by-product of copper ores obtained during the matte smelting and refining of copper [1, 2]. Sehi et al. [3] reported that copper slag is used in the manufacturing of cement and concrete, and Satpathy et al. [4] use copper slag as filler material in glass-epoxy composites for improvement in wear resistance properties. Similarly, red mud is the by-product of alumina obtained from bauxite by the Bayer's process. Red mud is used as a partial substitute of clay in ceramics products like bricks, tiles, and so on; it is also used in soils for treatment of iron-deficient soils [5–7]. Geetha et al. [8] reported the synthesis of red mud reinforced Al356 alloyed composites. Similarly, Mahata et al. [9] confirmed the fabrication of aluminum titanate–mullite composite from red mud rich in titanium. Fly ash is generated by coal combustion, and is composed of fine particles that are driven out of the boiler with the flue gases. Fly ash has been used as spherical filler for the production of lightweight high-strength concrete as well as fly ash reinforced metal or polymer composites [10, 11]. Rice milling generates a by-product know as husk. Alaneme et al. [12] reported the synthesis of rice husk ash reinforced Al–Si alloy composites and observed the effect of reinforcement on mechanical properties. Similarly, Narasaraju et al. [13] confirmed the synthesis of rice husk and fly ash reinforced hybrid Al–Si alloy composites and its mechanical properties. Again Debnath et al. [14] reported the adhesive and wear behavior of rice-husk-filled glass/epoxy composites.

Stone sector industries produce a huge amount of slurry by cutting or polishing of marble and granite slab. The waste marble slurry is converted into low-grade gypsum which is used in cement and fertilizer industries. The waste granite slurry is used in construction industries. Granite slurry or dry powder is a mixture of different oxides (SiO_2, Al_2O_3, etc.), and its chemical composition is presented in Table 11.1 [15]. Granite slurry is widely used in construction industries as a substitute of cement [16]. Granite powder has significant mechanical properties reported in Table 11.2 [15]. Kukshal et al. [17] evaluated the mechanical and fracture behavior of SiC-reinforced A356 alloy composites fabricated through liquid stir casting technique. Mechanical characterization results show that the hardness, tensile strength, and flexural strength

Table 11.1 Chemical composition of aluminum alloy 5083 [15]

Element	Al	Si	Fe	Cu	Mn	Mg	Zn	Ti	Cr
wt%	Balance	0.4	0.4	0.1	0.4–1	4.0–4.9	0.25	0.15	0.25

Table 11.2 Chemical composition of granite powder [15]

Element	SiO_2	Al_2O_3	K_2O	Na_2O	CaO	FeO	Fe_2O_3	MgO	TiO_2	MnO
wt%	72.04	14.42	4.12	3.69	1.82	1.68	1.22	0.71	0.30	0.05

of A356 alloy are enhanced by the addition of micro SiC particulates. However, the stress intensity factor was not of much effect with increment in crack length irrespective of particulate content. Similarly, in another study with alumina particles with the same alloy composite, the experimental result shows that the increment in alumina content in A356 alloy significantly affects the tensile strength, flexural strength, fracture strength, and Young's modulus [18]. Again, Gangwar et al. [19] examined the effect of TiO_2 particulate on mechanical properties of A380 alloy. The mechanical characterization results depicted that increment of titania particulates in A380 alloy enhanced the hardness and tensile strength, whereas the flexural strength is shown in reverse trend. Okayasu et al. [20] examined the effect of silicon nitride on mechanical properties of aluminum alloy. They reported that an increment of silicon nitride particulates in aluminum alloys degrades the bending strength of alloyed composites. Similar observation was also reported by Anilkumar et al. [21]. They showed the effect of fly ash content and particle size on mechanical properties of aluminum alloy. The experimental results show that the increment in fly ash particles into aluminum alloy enhanced compression strength, flexural strength, tensile strength, and hardness. On the other side, increment in fly ash particle size shows decrement in compression strength, tensile strength, flexural strength, and hardness of aluminum alloy. These composites materials were used in different fields, such as automobile, wind turbine, and structural building construction.

The present research work is focused on the gainful utilization of stone industry waste as filler. The chemical composition of granite powder shows that it is a mixture of different hard abrasive particles, such as alumina, silica, and iron oxides. These hard ceramic particles impart good strength and low thermal expansion coefficient at high temperature. A series of granite-reinforced aluminum alloy composites is fabricated through liquid stir casting technique. In composite series the aluminum alloy 5083 is mixed with different weight fractions (0, 2, 4, and 6 wt% granite particulate powder) of granite powder. Thereafter, physical, mechanical, fracture, and thermomechanical properties are determined for granite powder reinforced aluminum alloy composites.

Materials and Methods

In the present research work, we used aluminum alloy 5083 as matrix material and waste granite particulate powder as reinforcement. The mechanical properties and chemical composites of granite powder are presented in Tables 11.1 and 11.2 [15]. The designed formulations are fabricated using high-temperature vacuum casting machine (Fig. 11.1). A sequence of activities performed for fabrication are listed as follows:

1. The graphite crucible is preheated (about 200 °C) first to prevent oxidation of base material (i.e. aluminum alloy) and its easy melting.

Fig. 11.1 High-temperature vacuum casting machine and cast iron mold

2. Thereafter pieces of base material are put inside the crucible. Further, the crucible is heated till 650 °C. This melts the base material.
3. The reinforcing phase (i.e. granite powder) is added to the molten base alloy slowly and a mechanical stirrer at 400 rpm is used to mix the ingredients at least for 5 min. To ensure proper wettability between ingredients 1 wt% magnesium power is added to the mixture. This step continues for another 10 min. Thus, homogeneity in the mixture is ensured.
4. Now plunger is opened so that the molten metal is automatically poured into the molds (made of rectangular stainless steel) for solidification. The mold is kept in the room for around 20 min so as to achieve proper curing.
5. When the room temperature of casting is obtained, the specimen samples are prepared as per the characterization or testing methods with the help of diamond cutter.

Characterization Methods

In physical characterization the effect of reinforcement on density and void content is evaluated. Theoretical density is calculated by Agarwal and Broutman [22] who proposed formula for experimental density by water dispersion principle. Void content is difference in ratio of theoretical and experimental. In mechanical characterization flexural, hardness, impact, and fracture tests were carried out.

Flexural strength is measured according to ASTM standard E290 using the universal testing machine (UTM) provided by Aimil Ltd., India. ASTM E290 standard configures that the cross-head speed should be maintained 1 mm/min during the test. The span length is taken as 40 mm during that test with sample dimension of $60 \times 10 \times 10\ \text{mm}^3$, respectively. Micro-hardness test is carried out using Vicker's hardness tester according to ASTM standard E-9.

ASTM E-23 standard was used to evaluate the impact strength using impact tester. The test specimen size as per the standard is $64 \times 12.7 \times 3.2\ \text{mm}^3$ with depth of notch 10.2 mm. Thermo-mechanical properties were carried out using dynamic mechanical analyzer provided by Perkin Elmer-8000. The test was conducted in the temperature range of 30–250 °C at constant frequency (1 Hz) under three-point bending configuration. A roller supported load point applied a static force of 1 N uniformly on the middle of material and to inhibit friction effects. The sample size for dynamic mechanical analysis test is $27.5 \times 10 \times 1.5\ \text{mm}^3$. The span length was kept 25 mm during the three-point bending test.

ASTM E-399 is used to evaluate stress intensity factor using universal testing machine provided by Aimil Ltd., India. Fracture test is conducted in mode-I condition with different crack lengths. These crack lengths were prepared in the middle of specimen using wire electrical discharge machine. After test, breaking load and stress intensity factor is determined using Eqs. 11.1 and 11.2 for different crack lengths samples.

$$K1 = \frac{P}{B\sqrt{W}}\gamma(\beta) \tag{11.1}$$

$$\gamma(\beta) = \frac{\sqrt{2}\tan\frac{\pi a}{2W}}{\cos\frac{\pi a}{2W}}\left[0.75 + 2.02\left(\frac{a}{W}\right) + 0.37\left(1 - \sin\frac{\pi a}{3W}\right)^3\right] \tag{11.2}$$

whereas K is the stress intensity factor, P is maximum load (stress), B is thickness of specimen, W is width of specimen and a is crack length. $\gamma(\beta) =$ function of crack length and specimen width.

Results and Discussion

Effect of Granite Reinforcement on Density and Void Content

The physical and mechanical properties of a particulate-reinforced metal alloyed composites were dependent on the weight ratio of matrix and reinforcement materials. These properties were strongly affected by proper distribution of reinforcement material in composites and interface bonding between matrix and reinforcement materials. The void plays a vital role to examine the mechanical properties of a composite. The voids act as stress concentration point which leads toward early deformation under

Table 11.3 Theoretical/experiment density and void content with composites designation

Designations	Measured density (g/cc)	Theoretical density (g/cc)	Voids content (%)
5083 GD-0	2.12	2.18	2.75
5083 GD-2	2.23	2.32	3.87
5083 GD-4	2.35	2.48	5.24
5083 GD-6	2.45	2.62	6.49

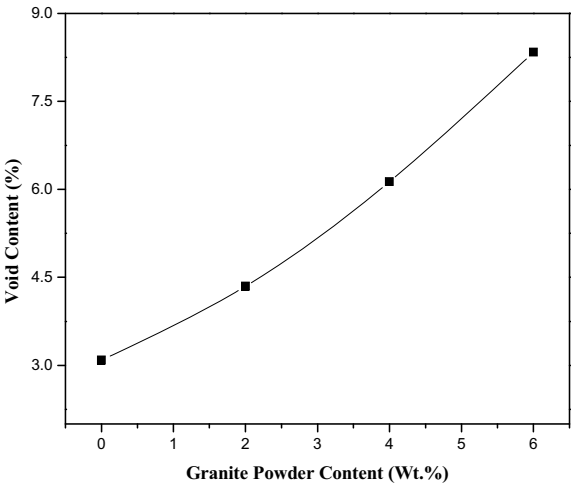

Fig. 11.2 Effect of granite powder reinforcement on void content of composites

the loading condition. The knowledge of void content was desirable for estimation of the quality of the composites. It was understandable that a good composite should have fewer voids. Table 11.3 shows the theoretical and experimental density with void content of granite powder reinforced aluminum metal alloy composites. It was observed from Fig. 11.2 that void content was increased with the addition of granite powder in alloy matrix material. The possible reason might be attributed to the fact that lower density may be attributed to insufficient bonding at the interface of matrix and ceramic particulates that left voids. The agglomeration of particulates while solidifying may have created intra-particulate voids because of insufficient bonding with matrix material. The possible error may be the fabrication methodology which resulted in voids contents [23].

Effect of Granite Reinforcement on Flexural Strength

Flexural strength of granite powder filled 5083 aluminum alloy composites is shown in Fig. 11.3. From Fig. 11.3 it was clearly observed that incorporation of granite powder into base matrix led to decrement in flexural strength of composites and the

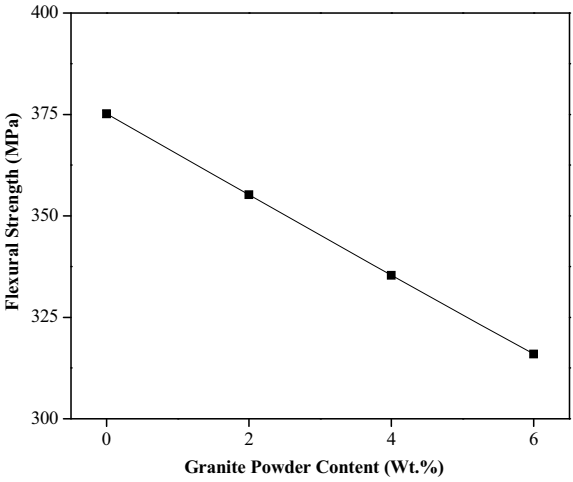

Fig. 11.3 Effect of granite powder reinforcement on flexural strength of composites

decrement rate was less. The flexural strength of aluminum alloy 5083 decreased up to ~19% after incorporation of granite particulate into base matrix. The maximum flexural strength 375.13 MPa and minimum flexural strength 315.93 MPa were obtained for 0 and 6 wt% granite-reinforced aluminum alloyed composites, respectively. From the analysis it was observed that the flexural strength decreases up to 5% by 2 wt% granite particulate incorporation into base matrix. It further decreased up to 6% on further addition of 2 wt% granite particulate and further decreased up to 6% on further addition of 2 wt% granite particulate into base matrix. The possible reason behind the degradation of flexural strength with incorporation of granite particulate into base matrix may lead to poor strength between the matrix and filler material, hence decreased the effectiveness of stress transfer between them [24–26].

Effect of Granite Reinforcement on Hardness

Figure 11.4 shows the hardness variation for granite powder reinforced aluminum alloy composites. From the graph it was observed that hardness is increased with the incorporation of granite powder into 5083 aluminum alloy. The hardness of pure 5083 aluminum alloy was found as 68 Hv, and after addition of 2 wt% granite powder it increased linearly ~12%. On further addition of 2 wt% granite powder it increased ~14%. On further addition of 2 wt% granite powder increased ~15% and the hardness was found to be 107 Hv. The reason behind the increment in hardness after addition of granite powder into base matrix may be that the granite powder was a mixture of different hard oxides. These hard oxides were dispersed into base matrix homogeneously and that would impart strength to base matrix. Similar results were reported by Park et al. [27] and Hunt et al. [28] for particulate-reinforced metal matrix composites.

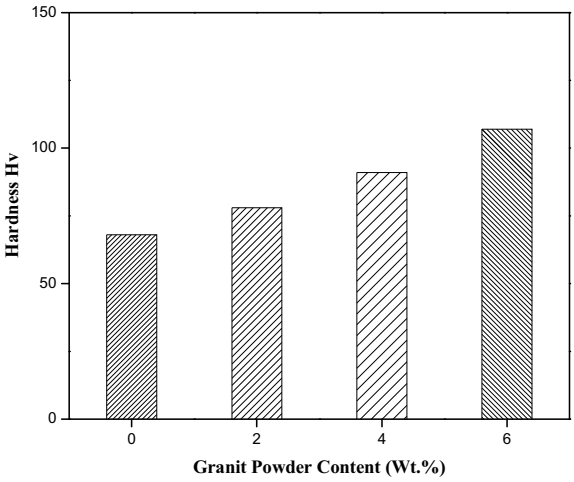

Fig. 11.4 Effect of granite powder reinforcement on hardness of composites

Effect of Granite Reinforcement on Impact Energy

Impact energy variation with reinforcement for 5083 aluminum alloy was presented in Fig. 11.5. From the graph it was observed that addition of granite particles improves the absorption of impact energy for aluminum alloy composites. The amount of energy absorption improved from 57 to 69 joules by incorporation of granite powder into base matrix. The percentage increase in impact energy from 2 to 6 wt% granite powder filled aluminum alloy composites were ~6, ~8, and ~4%, respectively. The possible reason behind the enhancement in impact energy may be the presence of hard abrasive particles in granite particulate which impart energy to soft matrix material.

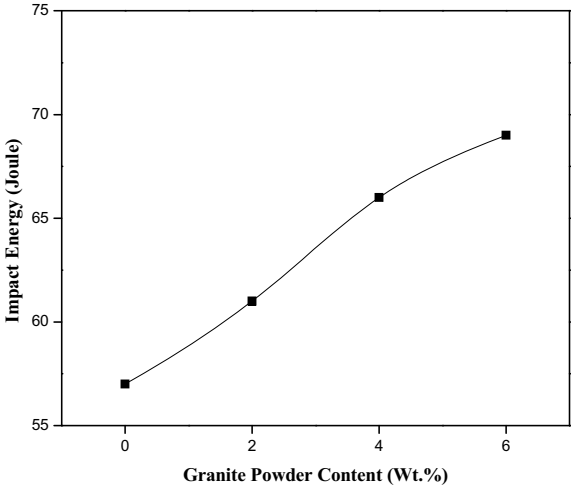

Fig. 11.5 Effect of granite powder reinforcement on impact strength of composites

These hard particles were responsible for the increment in the dislocation pile up and there was a restriction to the plastic flow. These results were in accordance with those obtained by Seah et al. [29], Sharma et al. [30], Kataih [31], which reported similar findings for particulate-filled metal matrix composites.

Effect of Granite Reinforcement on Stress Intensity Factor

The values of mode I stress intensity factors (SIFs) are calculated for granite powder filled aluminum alloy composites shown in Fig. 11.6. Figure 11.6 shows the variation of stress intensity factor with increment in granite particulate into 5083 aluminum alloy, as well as with increment in crack length. From the graph it is clearly observed that the stress intensity factor magnitude enhances with increment of granite particulate into 5083 aluminum alloy. The minimum stress intensity magnitude is obtained for 0 wt% granite-filled aluminum alloy composite and maximum stress intensity magnitude is obtained for 6 wt% granite-filled alloy composite. This may attribute to enhancement of interfacial bonding between matrix-particulates. In the literature it was reported that the magnitude of stress intensity factor is affected by several factors such as: the mechanical properties of the matrix and reinforcement, crack length, and loading conditions. The adhesion strength between the matrix and the reinforcement plays a significant role in determining the stress intensity factor at different crack lengths [32–36]. From the graph it was clearly depicted that the stress intensity factor magnitude is directly proportional to crack length. The crack growth behavior is significantly affected by several factors such as matrix material and reinforcement material. The amount of reinforcement material, their size and shape also affect the crack growth behavior. Hence, it was very difficult to conclude a specific cause, specifically particulate-filled alloy composites [32–36].

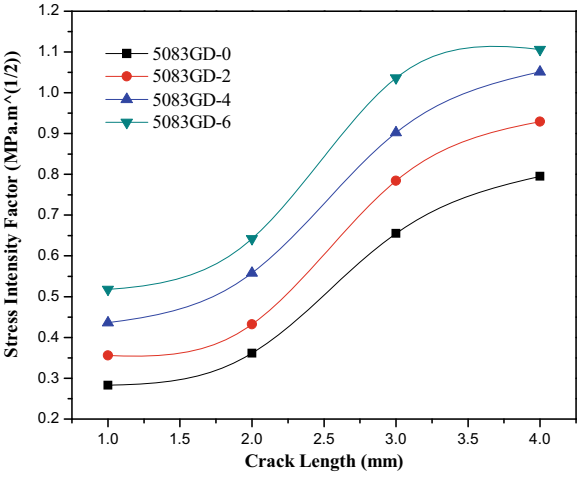

Fig. 11.6 Effect of granite powder reinforcement on stress intensity factor

Effect of Granite Reinforcement on Thermo-Mechanical Properties

Thermo-mechanical analysis of composites has been carried out to know the visco-elastic response of composites. To check the visco-elastic response the following properties were characterized, such as storage modulus (E'), loss modulus (E''), and damping factor (tan δ). These properties act as a function of temperature. The variation of E', E'', and tan δ are shown in Fig. 11.7a–c. Storage modulus (E') is known as the stiffness of visco-elastic material. Storage modulus (E') undergoes a consistent decay with increasing temperature in the range of 29–250 °C irrespective of the compositions. Figure 11.7a shows the variation of storage modulus (E') for granite particulate-reinforced aluminum alloyed composites. Figure 11.7a reveals that the storage modulus decays with increment in temperature, and a maximum decay in storage modulus was observed for 6 wt% granite powder reinforced composites. On the other hand, minimum decay in storage modulus is observed for granite particulate reinforced aluminum alloyed composites. The decay in storage modulus magnitude depends on the incorporation of granite powder particle as particle incorporated into base matrix enhanced stiffness of composites. The increase in E' in such cases may be ascribed to thermally induced phase transformations, leading to hardening of the composites. Similar observations are reported by Patnaik et al. [37] and Zang et al. [38] for particulate-reinforced metal alloy composites.

The loss modulus for granite particulate powder reinforced aluminum alloyed composites is shown in Fig. 11.7b. The graph reveals that with the increase in temperature, loss modulus magnitude is enhanced in the order of 6 wt% granite powder >4 wt% granite powder >2 wt% granite powder >0 wt% granite powder, respectively. Granite filler reinforcement was the main cause for proper flow of stress across the interface.

The damping factor (tan δ) indicates the amount of energy recovered in terms of mechanical damping or internal friction in visco-elastic system. The variation in tan δ of the composites as a function of temperature is shown in Fig. 11.7c for granite particulate powder reinforced aluminum alloyed composites. It is observed that the damping factor is directly proportional to temperature. High damping factor was obtained for granite powder reinforced composites when stiffness starts to decrease. The decrement in stiffness leads to the debonding between particulate and matrix material. The maximum damping factor is observed for 6 wt% granite powder and minimum for 0 wt% granite powder, respectively, for granite powder reinforced aluminum alloyed composites. Similar results were reported by Cox et al. [39] and Licitra et al. [40] for damping behavior of metal matrix composites.

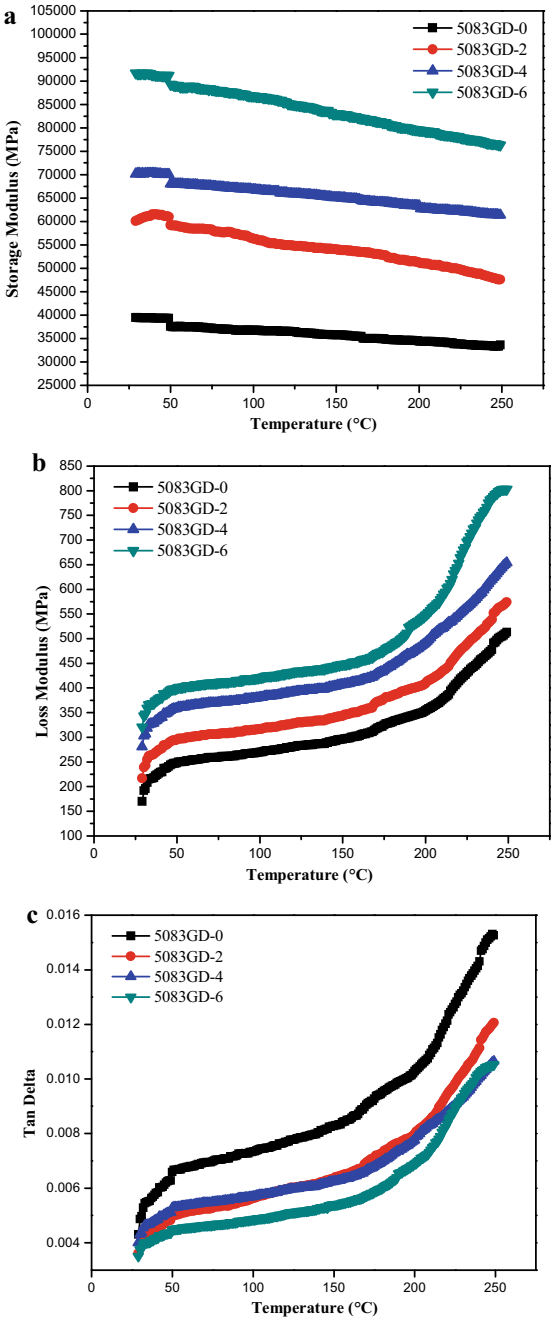

Fig. 11.7 **a** Variation of storage modulus with temperature for granite particulate powder reinforced aluminum alloyed composites, **b** variation of loss modulus with temperature for granite particulate powder reinforced aluminum alloyed composites, **c** variation of tan delta with temperature for granite particulate powder reinforced aluminum alloyed composites

Conclusion

This work shows that the stone industry waste, like granite powder, can be gainfully used as a potential cost-effective filler material for particulate-filled metal matrix composites. This work opens up a new avenue for value-added utilization of a solid industrial waste like granite powder. The following conclusions were drawn on the basis of fabrication and experimental results:

1. The granite powder filled aluminum metal matrix composites were fabricated successfully using stir casting technique with different weight fraction of filler material. Density and void test shows that density and void content of fabricated composites are enhanced with the incorporation of granite filler into 5083 aluminum alloy.
2. The addition of granite filler into 5083 aluminum alloy leads to the degradation of flexural strength. However, the maximum and minimum flexural strength was observed for unfilled aluminum alloy and 6 wt% granite powder reinforcement aluminum alloy composites.
3. Hardness and impact energy enhanced with the incorporation of granite filler into 5083 aluminum alloy. The maximum hardness and impact strength was found for 6 wt% granite powder aluminum alloy composites.
4. The magnitude of stress intensity factor enhanced with increment of granite filler into 5083 aluminum alloy as well as increment in crack lengths. However, 6 wt% granite powder filled composites shows maximum magnitude of stress intensity factor and unfilled aluminum alloy shows minimum stress intensity factor.
5. The visco-elastic properties of 5083 aluminum alloy were significantly altered by incorporation of granite filler in base matrix.

References

1. Biswas AK, Davenport WG (2003) Extractive metallurgy of copper. Pergamon Press, New York, p 518
2. Pati PR, Satapathy A (2015) Development of wear resistant coatings using LD slag premixed with Al_2O_3. J Mat Cycl Wast Manag 17:135–143
3. Shi C, Meyer C, Behnood A (2008) Utilization of copper slag in cement and concrete resources. Conserv Recycle 52:1115–1120
4. Biswas S, Satapathy A (2010) Use of copper slag in glass-epoxy composites for improved wear resistance. Wast Manag Res 28:615–625
5. Patel M, Padhi BK, Vidyasagar P, Pattnaik AK (1992) Extraction of titanium dioxide and production of building bricks from red mud. Res Ind 37(3):154–157
6. Summers RN, Guise NR, Smirk DD (1993) Bauxite residue (red mud) increases phosphorus retention in sandy soil catchments in Western Australia. Fertil Res 34(1):85–94
7. Satapathy A, Mishra SC, Ananthapadmanabhan PV, Sreekumar KP (2007) Development of ceramic coatings using redmud—a solid waste of alumina plants. J Sol Wast Techn Manag 33(2):48–53
8. Geetha B, Ganesan K (2014) Optimization of tensile characteristics of Al 356 alloy reinforced with volume fraction of red mud metal matrix composite. Proceedia Eng 97:614–624

9. Mahata T, Sharma BP, Nair SR, Prakash D (2000) Formation of aluminium titanate–mullite composite from bauxite red mud. Mater Mat Trans B 318:551–553
10. Sarajaadevi M, Murugesan V, Rengaraj K, Anamd P (1998) Utilization of fly ash as filler for unsaturated polyester resin. J Appl Poly Sci 69:1385–1391
11. Sharma KK, Swaroop S, Thakur DS (1993) Recycling of LD slag through sinter route on direct charging in blast furnace at Bhilai Steel Plant. In: Proceedings of national seminar on pollution control in steel industries, pp 72–79
12. Alaneme KK, Akintunde IB, Olubambi PA, Adewale TM (2013) Fabrication characteristics and mechanical behavior of rice husk ash-alumina reinforced Al-Mg-Si alloy matrix hybrid composites. J Mater Res and Tech 2(1):60–67
13. Narasaraju G, Raju DL (2015) Characterization of hybrid rice husk and fly ash-reinforced aluminium alloy (AlSi10Mg) Composites. Mater Toda Proceed 2:3056–3064
14. Debnath K, Dhawan V, Singh I, Dvivedi A (2014) Adhesive wear and frictional behavior of rice husk filled glass/epoxy composites. J Prod Eng 17(1):21–26
15. Gautam V, Patnaik A, Bhat IK (2015) Thermo-mechanical and fracture characterization of uncoated, single and multilayer (SiN/CrN) coating on granite powder filled metal alloy composites. Silic 8:133–143
16. Kala TF (2013) Effect of granite powder on strength properties of concrete. Inter J Eng Sci 2(12):36–50
17. Kukshal V, Gangwar S, Patnaik A (2013) Experimental and finite element analysis of mechanical and fracture behavior of SiC particulate filled A356 alloy composites: Part I. J Mat Des Appl 229:91–105
18. Kukshal V, Gangwar S, Patnaik A (2013) Experimental and finite element analysis of mechanical and fracture behavior of Al_2O_3 particulate-filled A356 alloy composites: part II. J Mat Des Appl 229:64–76
19. Okayasu M, Hitomi M, Yamazaki H (2009) Mechanical and fatigue strengths of silicon nitride ceramics in liquid aluminum alloys. J Eur Ceram Soc 29:2369–2378
20. Gangwar S, Patnaik A (2013) A study on the physical and mechanical properties of TiO_2 filled A380 alloy composites. Inter J Comp Mat 3:69–72
21. Anilkumar HC, Hebbar HS, Ravishankar KS (2011) Mechanical properties of fly ash reinforced aluminium alloy (al6061) composites. Inter J Mech Mat Eng 6:41–45
22. Agarwal BD, Broutman IJ (1990) Analysis and performance of fiber composites, 2nd edn. Wiley, New York
23. Turk A, Durman M, Kayali ES (2007) The effect of manganese on the microstructure and mechanical properties of zinc-aluminium based ZA-8 alloy. J of Mater Sci 42:8298–8305
24. Chu S, Wu R (1999) the structure and bending properties of squeeze-cast composites of A356 aluminium alloy reinforced with alumina particles. Comp Sci and Tech 59:157–162
25. Abdullah Y, Razak Y, Daud RS, Harun M (2009) Flexural strength and fracture studies of Al-Si/SiC_p composites. IJMME 4:109–111
26. Qu Z, He R, Wei K, Pei Y, Fang D (2015) Pre-oxidation temperature optimization of ultra-high temperature ceramic components: flexural strength testing and residual stress analysis. Cera Inter 41(3):5085–5092
27. Park BG, Crosky AG, Hellier AK (2008) High cycle fatigue behaviour of microsphere Al–Al_2O_3 particulate metal matrix composites. Comp: Part B 39:1270–1279
28. Seah KHW, Sharma SC, Girish BM, Kamath R, Satish BM (1997) Mechanical properties and fractography of cast lead/quartz particulate composites. Mater and Des 18(3):149–153
29. Sharma SC (1997) Mechanical properties and fractography of cast lead/quartz particulate composites. Mater Des 18:149–153
30. Kataiah GS, Girish DP (2010) The mechanical properties and fractography of aluminium 6061-TiO_2 composites. Int J Pharm Stud Res 1:17–25
31. Papakyriacou M, Mayer HR, Stanzl SET, Groschl M (1995) Near-threshold fatigue crack growth in Al_2O_3 particle reinforced 6061 aluminium alloy. Fat Frac Eng in Mater struc 18(4):477–487

32. Levin M, Karlsson B (1991) Influence of SiC particle distribution and prestraining on fatigue crack growth rates in aluminium AA6061-SiC composite material. Mater Sci and Tech 7:596–607
33. Kumai S, Yoshida K, Higo Y, Nunomura S (1996) Effects of dendrite cell-size and particle distribution on the near-threshold fatigue-crack growth-behavior. Acta Mater 44(6):2249–2257
34. Somekawa H, Kim HS, Singh A, Mukai T (2007) Fracture toughness in direct extruded Mg-Al-Zn alloys. J Mater Res 22:2598–2607
35. Hemanth J (2001) Fracture toughness and wear resistance of Aluminum-boron particulate composites cast using metallic and non metallic chills. Mater Des 23:41–50
36. Zong BY, Zhang F, Wang G, Zuo L (2007) Strengthening mechanism of load sharing of particulate reinforcements in a metal matrix composite. J Mater Sci 42:4215–4226
37. Patnaik A, Mamatha TG, Biswas S, Kumar P (2012) Damage assessment of titania filled Zinc-aluminum metal matrix composites in erosive environment: a comparative study. Mater and Des 36:511–521
38. Zhang JM, Perez RJ, Wong CR, Lavernia EJ (1994) Effects of secondary phases on the damping behavior of metals, alloys and metal-matrix composites. Mater Sci Eng 13:325–389
39. Cox J, Luong DD, Shunmugasamy VC, Gupta N, Strbik OM, Cho K (2014) Dynamic and thermal properties of aluminum alloy A356/silicon carbide hollow particle syntactic foams. Meta 4:530–548
40. Licitra L, Luong DD, Strbik OM, Gupta N (2015) Dynamic Properties of alumina hollow particle filled aluminum alloy A356 matrix syntactic foams. Mater Des 66:50–55